J. Phys.: Condens. Matter **24** (2012) 305801 (8pp) doi:10.1088/0953-8984/24/30/305801

The relationship between hydrogen and paramagnetic defects in thin film silicon irradiated with 2 MeV electrons

O Astakhov[1,2], R Carius[1], Yu Petrusenko[2], V Borysenko[2], D Barankov[2] and F Finger[1]

[1] Forschungszentrum Jülich, IEK-5, 52425 Jülich, Germany
[2] National Science Center Kharkov Institute of Physics and Technology, CYCLOTRON Facility, Akademichna 1, 61108 Kharkov, Ukraine

E-mail: o.astakhov@fz-juelich.de

Received 14 March 2012, in final form 12 June 2012
Published 4 July 2012
Online at stacks.iop.org/JPhysCM/24/305801

Abstract

After irradiation of hydrogenated amorphous and microcrystalline silicon (a-Si:H and μc-Si:H) with 2 MeV electrons at 100 K, we observe satellite-like components close to the dominating electron spin resonance (ESR) signal of these materials. The satellites overlap with the commonly observed dangling bond resonance and are proposed to originate from a hyperfine interaction with the nuclear magnetic moment of hydrogen atoms in a-Si:H and μc-Si:H. Our present study is focused on the verification of this hypothesis.

Equivalent hydrogenated and deuterated a-/μc-Si:H/D materials have been investigated with ESR before and after 2 MeV electron bombardment. From the difference between ESR spectra of hydrogenated and deuterated samples we identify the doublet structure in the ESR spectra as a hyperfine pattern of hydrogen-related paramagnetic centers. The observations of H-related paramagnetic centers in a-/μc-Si:H are of particular interest in view of metastability models of a-Si:H, which include H-related complexes as precursors for the stabilization of the metastable Si dangling bonds.

The nature of the observed center is discussed in the light of known H-related complexes in crystalline Si and suggested H-related dangling bonds in a-Si:H.

(Some figures may appear in colour only in the online journal)

1. Introduction

Hydrogenated thin film silicon, commonly deposited from the gas phase, is a class of materials which includes microcrystalline (μc-Si:H) and amorphous (a-Si:H) silicon. As a consequence of structural disorder these materials possess a high density of silicon dangling bonds (dbs). In hydrogenated material most of these dangling bonds are passivated by hydrogen, leaving typically only 10^{15}–10^{16} db cm^{-3} unsaturated [1]. This results in material with an electronic quality appropriate for application in solar cells and other thin film devices. Hydrogen, being therefore on the one hand of advantage to reduce the defect density, is on the other hand related to metastability phenomena in a-Si:H such as creation of additional metastable dangling bonds under illumination (Staebler–Wronski effect, SWE [2]) or under bias voltage [3]. It is proposed that H takes part in the production and the stabilization of metastable dangling bonds [4]. Various models for the mechanism of the SWE include hydrogen migration and, at least temporary, existence of H-related defect complexes. These are e.g. hydrogen-related db (H–db) in the 'Stutzmann–Jackson–Tsai' model [5] or bond centered hydrogen (BC-H) in the 'hydrogen collision' model [6]. Experimental evidence for the existence of H-related defects and information on their structure is of importance for the understanding of SWE, which is nowadays rigorously examined with sophisticated

experimental techniques combined with simulations [7] and *ab initio* calculations [8].

Electron spin resonance [9] is a suitable method for the investigations of H-related centers in a-Si:H. ESR is sensitive to the unpaired (paramagnetic) electrons localized in defect states of a semiconductor [10, 11]. Among interactions of paramagnetic electrons with their nearest environment the spin–orbit coupling (described by the g-tensor [9]) and hyperfine coupling between electron spin and nuclear spin (described by the A-tensor [9]) are of major importance in conventional ESR [12]. For the investigation of H-related centers the hyperfine (HF) interaction is of particular interest given that a proton possesses a nonzero nuclear spin I [13]. Hyperfine interaction is observed in ESR spectra as a splitting of the spectral lines. If a paramagnetic complex contains an atom with nonzero nuclear spin the number of hyperfine lines along with the magnitude of hyperfine splitting in the ESR spectra help to identify the nucleus. A variety of hydrogen-related defects have been identified with analysis of the hyperfine structures in the ESR spectra of crystalline silicon (c-Si) [14–17]. In the case of H ($I = 1/2$) the resonance line is split in $2I + 1 = 2$ hyperfine transitions. Replacement of H with its isotope deuterium (D, $I = 1$) leads to the splitting of the spectral components into three HF lines. This isotope replacement is commonly used in order to examine the presence of H in the paramagnetic complex of interest [18]. The diversity in the hyperfine pattern after H $\rightarrow$ D replacement caused by the higher spin number I of D facilitates assigning the observed HF pattern to H [14–17].

Taking into account the high concentration of H (around 10 at.%) in both a-Si:H and μc-Si:H, one can expect hydrogen induced hyperfine patterns in the ESR spectra of these materials. However, in numerous ESR studies conducted on μc-Si:H and a-Si:H [19–25] the spectrum was dominated by a featureless single line of dangling bonds with no evidence for the expected hydrogen induced HF splitting. These results question the existence of paramagnetic states with H in the immediate vicinity in a-Si:H or μc-Si:H. H-related states however are often used for the explanation of metastable defect creation [4]. In this connection, several attempts have been made to determine the minimum distance between the H atom and db in a-Si:H. It was claimed to be about 4 Å by Isoya *et al* [23, 24]. With ENDOR [26] and EDMR [27] experiments on a-Si:H 'distant hyperfine interaction between the ensembles of dangling bond defects and hydrogen nuclei was detected. No resolved ligand hyperfine structure was found' [27]. In a more recent work by Fehr *et al* [28], a continuous distribution of distances between H nuclei and dbs is suggested, including distances even shorter than 3 Å.

In view of the experimental findings and the suggested models, unambiguous experimental evidence for hydrogen induced hyperfine pattern in the ESR spectra of a-Si:H or μc-Si:H would be of major interest.

In our former studies of the role of defects in the electronic properties of a-Si:H and μc-Si:H, the material has been exposed to 2 MeV electron bombardment at 100 K in order to increase the defect density. After the bombardment we observed satellite-like features on the wings of db resonance in the ESR spectra of both a-Si:H and μc-Si:H [29–31]. In the present paper the nature of these satellites is examined with H $\rightarrow$ D isotope exchange experiments. ESR measurements of the virtually identical hydrogenated/deuterated a-Si:H/D and μc-Si:H/D indicate that the features in the spectra of the irradiated material belong to a hydrogen-related hyperfine pattern. The nature of this center is discussed in the light of known H-related complexes found in c-Si [14–17] and suggested H-related db states in a-Si:H [32, 33].

2. Experiment

Samples of a-Si:H and μc-Si:H were deposited with VHF-PECVD at 185 °C on Mo foil from a mixture of silane and hydrogen ($SiH_4 + H_2$) [34, 35] and a mixture of deuterated silane and deuterium ($SiD_4 + D_2$). The silane to hydrogen ratio (silane concentration—SC = $SiH_4/(SiH_4 + H_2)$ or $SiD_4/(SiD_4 + D_2)$) was varied from 3 to 100% to obtain material with different crystalline volume fractions I_C evaluated from Raman spectra [36]. Raman spectra were measured at room temperature with laser excitation at $\lambda =$ 647 nm. The crystalline volume fraction is considered to be constant throughout the whole experimental procedure.

Samples were irradiated in quartz tubes with 2 MeV electrons at 100 K up to a dose of 1.1×10^{18} e cm^{-2} at a rate of about 3×10^{13} e cm^{-2} s^{-1}. The sample tubes were handled, transported and stored in liquid nitrogen (LN_2). X-band CW ESR was measured at 40 K for improved signal-to-noise ratio. More details on the experiment are given elsewhere [29, 30, 37, 38].

3. Results

3.1. Experimental results

The g-value and the spin density N_S, determined from the dangling bond ESR line of thin film silicon samples, are plotted versus silane concentration in figure 1. Two series of samples, hydrogenated and deuterated, have been prepared at nominally identical conditions. The samples of the deuterated material are shown with filled symbols. The transition between microcrystalline and amorphous material is shown with a gray vertical line (SC $\approx$ 8%) defined according to the results of Raman spectroscopy. There is a shift of the g-value between highly crystalline and amorphous samples, in agreement with our earlier studies [37, 38]. The shift with increase of SC also takes place within the Raman amorphous range (SC = 8–100%). N_S has a minimum in the Raman amorphous range at SC = 10–20%, which corresponds to high material quality appropriate for e.g. high efficiency solar cell preparation. Further increase in SC leads to increases in deposition rate and defect density. Both hydrogenated and deuterated materials have very similar properties as for ESR, conductivity and Raman spectroscopy prior to the electron bombardment.

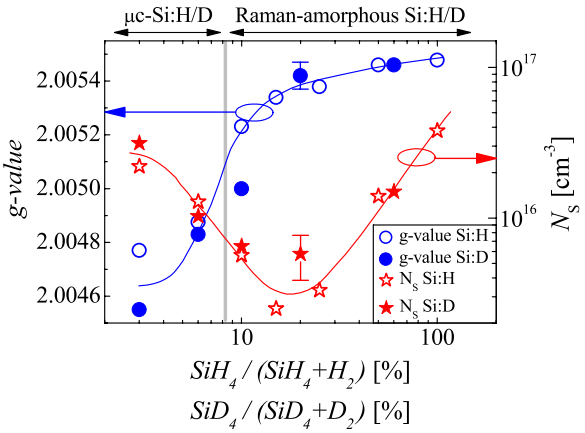

Figure 1. *g*-value (blue circles) and spin density (red stars) versus silane concentration for the as-deposited a-Si:H/D and μc-Si:H/D. The data obtained on the deuterated samples are shown with filled symbols. The gray vertical line separates material which does or does not show crystalline components in the Raman spectrum. The solid lines are guides for the eye.

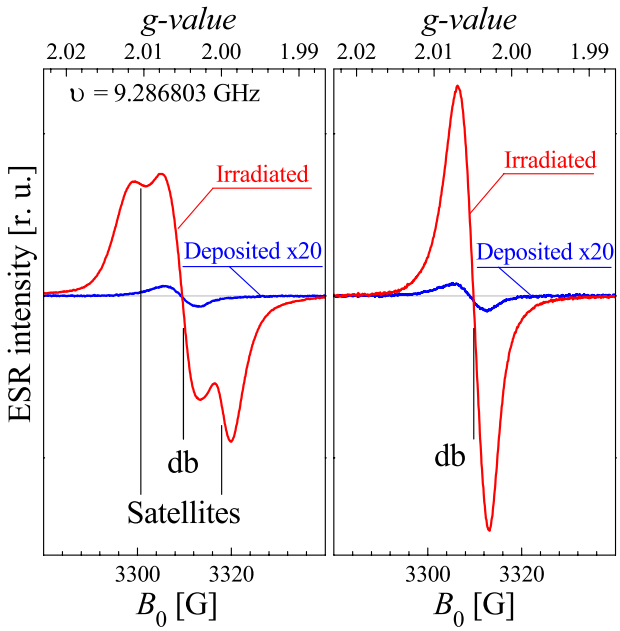

Figure 2. ESR spectra measured before and after 2 MeV electron bombardment in (a) a-Si:H and (b) a-Si:D prepared at SC = 10%.

The difference between the ESR spectra of the hydrogenated and deuterated material after electron bombardment is demonstrated for a-Si:H and a-Si:D samples prepared at SC = 10% in figure 2. Initial 'as-deposited' (magnified by a factor of 20) spectra consist of the dangling bond resonance and have the same shape and position in both a-Si:H and a-Si:D. After the e bombardment the intensity of the ESR lines increases by three orders of magnitude from $N_S = 3 \times 10^{15}$ to 10^{18} cm^{-3} in both a-Si:H and a-Si:D due to the strong increase in defect density. The difference in the shape of resonances after the electron bombardment is obvious. Satellite-like features on the wings of the db resonance in a-Si:H are observed, in agreement with our earlier works [29–31]. Clearly, these satellites are absent from the resonance of a-Si:D irradiated under the same conditions. The difference in the spectra is apparently due to the isotope exchange of H with D.

The satellites and corresponding H → D isotope exchange effect are observed after e bombardment over a broad range of the material structures, i.e. a-Si:H/D and μc-Si:H/D with various crystallinities, as shown in figure 3. The density of paramagnetic defects has been increased by two to three orders of magnitude for different material structures after electron bombardment [29, 30]. In order to compare the shape of the resonances before and after irradiation, the spectra in figure 3 were adjusted to the same amplitude. Spectra of the irradiated hydrogenated material in figure 3(a) contain satellite humps on the wings of the db resonance over a broad range of SC from highly crystalline μc-Si:H to a-Si:H. These satellites are observed most clearly in the spectra of a-Si:H prepared at SC of 10 . . . 20%. At SC beyond 20% the fraction of the satellites becomes smaller with increasing SC and is no longer visible at SC = 100%. On the other hand, the spectra of deuterated material in figure 3(b) do not contain the doublet features after the electron bombardment. In addition to the satellite doublet that is sensitive to H → D exchange, one more spectral feature is observed in the low field part of the ESR lines after irradiation for both hydrogenated and deuterated μc-Si:H/D. The resonance contribution is labeled as C in figure 3. The additional signal C at $g \approx 2.006$–2.008 brings considerable asymmetry to the spectra. Note that a similar shape of the ESR lines has been found in the spectra of μc-Si:H after exposure to atmospheric gases [39]. Speculatively, the component C had been connected with defect states in different environments of the microcrystalline silicon phase, i.e. bulk versus grain boundaries. Since this feature is not sensitive to the H → D isotope replacement, we shall not consider it further for the evaluation of the results in the present work.

Based on the observed isotope exchange effect the doublet of satellites in the spectra of irradiated a-Si:H and μc-Si:H is interpreted as a hydrogen-related hyperfine pattern overlapped with the commonly observed db resonance. The corresponding hyperfine triplet in the deuterated samples is not resolved in figures 2(b) and 3(b) because the nuclear *g*-value of D is about one-sixth that of H [13]. This implies a proportionally smaller splitting of the HF lines. These closely standing lines are not resolved from the overlapping strong db resonance.

3.2. Spectrum analysis and simulation

In order to extract the parameters of the paramagnetic center responsible for the observed HF pattern, a detailed spectrum analysis is required. Principal values of the *g*-tensor and *A*-tensor are of interest here. However, there are two factors that are obstacles to the direct extraction of these values from the measured spectrum.

At first the hyperfine doublet overlaps with the db resonance. For the spectrum analysis we assume that

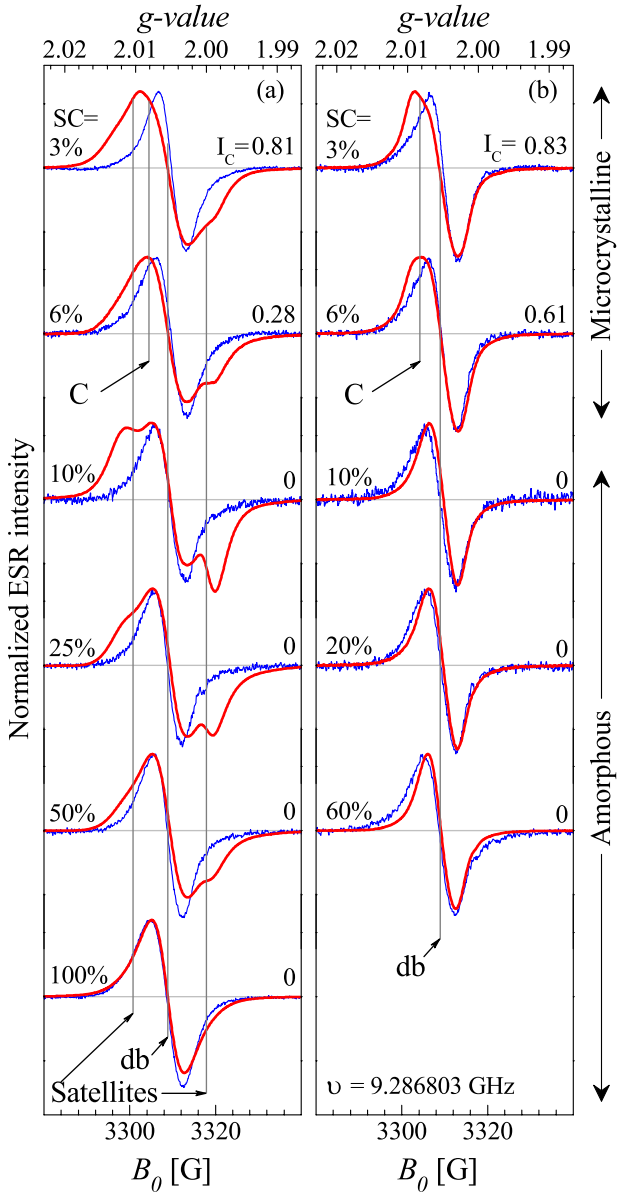

Figure 3. ESR spectra of hydrogenated (a) and deuterated (b) thin film silicon. For each sample a pair of spectra is presented: before (thin blue lines) and after (bold red lines) electron bombardment. All spectra are normalized to the same amplitude for the line shape comparison. The spectra are lined up according to SC of the samples. The vertical lines indicate the position of the db resonance and the approximate positions of an additional resonance feature (noted as C) after the electron bombardment. The values of the silane concentration and the Raman crystallinity are given for each sample.

the measured spectrum on a magnetic field scale is a linear combination of the dangling bond resonance db(B) and the hyperfine pattern hfs(B). These components taken with corresponding scaling factors α and β compose the measured spectrum $Y_{\mathrm{ESR}}(B)$ as follows:

$$Y_{\mathrm{ESR}}(B) = \alpha \mathrm{db}(B) + \beta \mathrm{hfs}(B). \quad (1)$$

The $Y_{\mathrm{ESR}}(B)$ term is the measured spectrum and is known per definition. The dangling bond component db(B) is assumed to have the same shape as the db line before the sample irradiation, but with increased intensity due to enhanced density of db states. This assumption is based on the following arguments

- The excess paramagnetic defects created with 2 MeV electron bombardment at 100 K start to anneal at room temperature and can be annealed out completely at 160 °C [30, 31]. At the same time the intensities of the hyperfine satellites decay faster than the intensity of the central resonance upon stepwise annealing [30]. This results in spectra with already annealed-out satellites, but a db line with a still much higher intensity as compared with the initial level. For this central db line we find no shape or position variations with intensity before and after irradiation.
- In the spectra of a-Si:H prepared intentionally of poor quality at SC = 100% the hyperfine satellites were not resolved. In this case very few variations in the shape of db resonance are observed after electron bombardment in comparison to the initial resonance (figure 3).
- The spectra of the deuterated amorphous silicon after the electron bombardment are very similar to the initial db resonances (figure 3).

We therefore assume that the resonance of dbs, at least in a-Si:H/D, does not change its shape and position, while its intensity increases strongly after the electron bombardment. The spectrum measured before the electron bombardment is taken as db(B).

In contrast to the measured spectrum $Y_{\mathrm{ESR}}(B)$ or dangling bond component db(B), neither hfs(B) nor the scaling factors α and β are known or can be defined under reasonable assumptions. Therefore hfs(B) cannot be extracted and analyzed directly. Instead one can take the spectra as reported in the literature for hydrogen-related centers found in crystalline silicon or for the states predicted for a-Si:H, combine them with the dangling bond resonance db(B), and investigate the agreement of such a linear combination with the measured spectrum $Y_{\mathrm{ESR}}(B)$ in terms of e.g. a correlation coefficient.

However, the spectra reported for crystalline silicon cannot be directly applied as hfs(B), because the structural disorder of a-Si:H/D and μc-Si:H/D has to be taken into account. This structural disorder leads to an inhomogeneous broadening (strains in g-tensor and A-tensor values) and angular averaging of the spectra [9, 20] that in turn smears out the fine structure of the spectrum. The angular averaging leads to a specific powder spectrum [20], which can be simulated [20, 40, 41] using the principal values of the g-tensor and A-tensor measured in a crystal. The inhomogeneous broadening is accounted for in our simulations via the degree of g-strain and A-strain. For convenience in the present simulation the g-strain has been chosen arbitrarily as the dominant contribution (see the appendix). Note that equivalent results are obtained with a dominant A-strain. The software tool *EasySpin* [42] has been applied for the powder spectrum simulations. The whole analysis chain has been divided into two steps. First, using

the parameters reported in the literature, the powder spectrum hfs(B) has been simulated with *EasySpin*. In the second step the ratio of the scaling coefficients α/β is optimized to obtain the best correlation of [αdb(B) + βhfs(B)] with $Y_{\mathrm{ESR}}(B)$.

The correlation between the sum [αdb(B) + βhfs(B)] and the measured spectrum $Y_{\mathrm{ESR}}(B)$can be evaluated e.g. with Pearson's correlation coefficient r [43]. Note however that the correlation coefficient r between the pure db component db(B) and the spectrum measured after irradiation $Y_{\mathrm{ESR}}(B)$ is already relatively high at $r_{\mathrm{db}} = 0.79$. Since the component db(B) remains unchanged in the simulation procedure, it is more convenient to evaluate the impact of hfs(B) only, using the following parameter:

$$r' = \frac{r - r_{\mathrm{db}}}{1 - r_{\mathrm{db}}} \qquad (2)$$

where r is a Pearson's correlation coefficient between [αdb(B) + βhfs(B)] and $Y_{\mathrm{ESR}}(B)$, and r_{db} is a coefficient of correlation between db(B) and $Y_{\mathrm{ESR}}(B)$ equal to 0.79. Thus r' determines to what extent hfs(B) improves the correlation between [αdb(B) + βhfs(B)] and $Y_{\mathrm{ESR}}(B)$ in comparison to the pure db(B) at given α/β-ratio. At $r' = 0$ there is no improvement and at $r' = 1$ the matching of [αdb(B)+βhfs(B)] to $Y_{\mathrm{ESR}}(B)$ is perfect.

Now we can apply the described procedure to the existing data. For $Y_{\mathrm{ESR}}(B)$ we take the spectrum of a-Si:H (SC = 10%) after electron bombardment, where the hyperfine pattern is most clearly observed (red spectrum on the left of figures 2, or 3 at SC = 10%). The spectrum of this sample measured before electron bombardment is taken for db(B) (blue spectrum on the left of figures 2 or 3 at SC = 10%). The results of simulation for different H-related centers in Si are taken as hfs(B).

For the simulations of hfs(B) we used all available literature where parameters of H-related paramagnetic states in Si are presented: several H-related paramagnetic centers observed in c-Si [14–17], and estimations for the H-related db complex suggested for a-Si:H [32, 33]. All of these centers listed in table 1 have anisotropic g- and A-tensors. Using these parameters, a powder pattern simulation for each center has been performed to obtain the hyperfine component hfs(B). The details of the simulations are summarized in the appendix. The results of the powder pattern simulation are presented in figure 4(a) with two curves for each H-related center. The narrow black line represents the spectrum with negligible broadening (very small g-strain), where the fine structure of the powder pattern can be seen. The blue (bold) spectra in figure 4(a) represent the same powder patterns calculated taking account of inhomogeneous broadening (g-strain of 0.0043) in the amorphous matrix. These spectra are taken as the hfs(B) component for each given H-related center. Next these spectra are combined with the resonance of the dangling bonds db(B) and the result [αdb(B) + βhfs(B)] is shown in figure 4(b). In each case the α/β-ratio has been optimized to obtain the highest r'. The measured reference spectrum $Y_{\mathrm{ESR}}(B)$ is shown behind each simulated curve for comparison. The parameters for simulation, α/β-ratio and r', are presented in table 1.

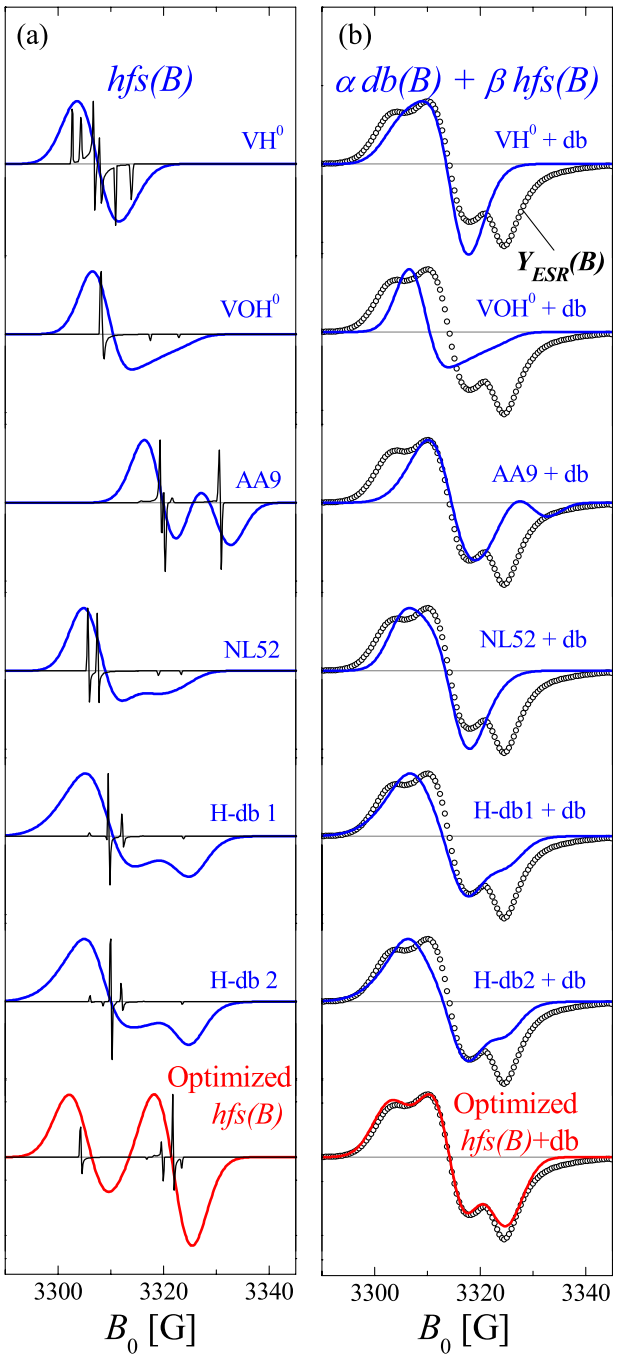

Figure 4. (a) Powder pattern simulations performed for different hydrogen-related centers. Bold blue lines represent the results of simulation taking account of the inhomogeneous broadening—hfs(B). The narrow black lines represent the fine structure of the spectra without considerable broadening. The last spectrum represented by the red line is the 'optimized hfs(B)'—powder pattern simulation of hfs(B) performed after optimization of the parameters of the axially symmetric g-tensor and A-tensor. (b) The sum αdb(B) + βhfs(B) for each simulated hfs(B) spectrum is shown with bold blue lines. The reference spectrum measured after electron bombardment $Y_{\mathrm{ESR}}(B)$ is shown with circles behind the simulated spectra.

From the comparison of [αdb(B) + βhfs(B)] with the reference $Y_{\mathrm{ESR}}(B)$ in figure 4(b), and from the correlation coefficient r' in table 1, it is evident that none of the spectra

Table 1. *g*-tensor, *A*-tensor, *g*-strain, α/β-ratio and correlation coefficient r' used to simulate powder spectra of diverse hydrogen-related centers.

Center	Description	g_1 *g*-strain	g_2 *g*-strain	g_3 *g*-strain	A1 (MHz)	A2 (MHz)	A3 (MHz)	α/β	r'	Reference
VH0	H atom in Si vacancy	2.009 0	2.011 4	2.006	−3.3	−4.6	−8.5	3.8	0.1	[15]
		0.004 3	0.004 3	0.004 3						
VOH0	H atom in O vacancy	2.008 4	2.008 6	2.001 3	−0.8	−0.3	15.2	2.2	0.08	[16]
		0.004 3	0.004 3	0.004 3						
AA9	Bond centered H	2.001 1	1.998 3	1.998 3	6.2	31.4	31.4	3	0.15	[14]
		0.0043	0.004 3	0.004 3						
NL52	H quasimolecule in Si vacancy	2.000 7	2.0095	2.009 5	12.1	5.0	5.0	1.7	0.2	[17]
		0.004 3	0.004 3	0.004 3						
H–db[a]	H-related db (a-Si:H)	2.003 5	2.0069	2.006 9	40.7	7.3	7.3	0.89	0.59	[33]
		0.003 84	0.008 76	0.008 76						
H–db	H-related db (a-Si:H)	2.003 8	2.006 8	2.006 8	42.1	5.6	5.6	0.89	0.61	[32]
		0.003 36	0.008 93	0.008 93						
	Optimized hfs(*B*)	2.002 4	2.0056	2.005 6	8.4	49.1	49.1	2	0.97	
		0.005	0.005	0.005						

[a] The values are averaged for all samples presented in [33].

simulated with the data from the literature can represent the features of a measured spectrum $Y_{\mathrm{ESR}}(B)$ satisfactorily. The best result with $r' = 0.61$ is obtained with a simulation using parameters suggested for an H–db complex [32]. In summary, the described simulation procedure does not allow us to unambiguously identify the HF pattern observed in a-Si:H after the electron bombardment as one of the reported H-related centers listed in table 1.

As the ESR spectra simulated with parameters of the reported H-related centers fail to represent the measured spectrum adequately, we can try to adjust the principal values of *g*- and *A*-tensors in order to obtain a better agreement with experiment. For the hyperfine pair we use axially symmetric *A*- and *g*-tensors, which are co-linear for simplicity, and simulate the powder pattern hfs(*B*). The simulated hfs(*B*) is then combined with db(*B*) and the sum $[\alpha\mathrm{db}(B) + \beta\mathrm{hfs}(B)]$ is compared with the reference $Y_{\mathrm{ESR}}(B)$ in the same way as described above. The principal values of axially symmetric *g*- and *A*-tensors used for the simulation of hfs(*B*) have been optimized iteratively in order to improve r' between $[\alpha\mathrm{db}(B)+\beta\mathrm{hfs}(B)]$ and $Y_{\mathrm{ESR}}(B)$. The spectra simulated with optimized parameters of *g*-tensor and *A*-tensor are presented by red lines at the bottom of the figures 4(a) and (b) denoted as 'optimized hfs(*B*)'. It was possible to achieve good correlation ($r' = 0.97$) between $[\alpha\mathrm{db}(B) + \beta\mathrm{hfs}(B)]$ and $Y_{\mathrm{ESR}}(B)$. The parameters of *g*- and *A*-tensors for optimized hfs(*B*) are shown in the last row of table 1.

Staying within the assumptions made for the spectrum simulations we can deduce some of the properties of the hypothetic H-related complex behind the HF-pair spectrum. The isotropic and anisotropic HF components of the hypothetic center are $A_{\mathrm{iso}} = (A_{\parallel} + 2A_{\_|\_})/3 = 35.5$ MHz, $A_{\mathrm{aniso}} = (A_{\parallel} - A_{\_|\_})/3 = 13.5$ MHz respectively. The isotropic term A_{iso} used for evaluation of an electron probability density at the paramagnetic nucleus

$$|\psi(0)|^2 = \frac{3\hbar A_{\mathrm{iso}}}{2\mu_0 g\beta\beta_N} \tag{3}$$

gives $|\psi(0)|^2 = 3.76$ electron Å^{-3}.

The point dipole approximation commonly used to estimate the distance *R* between magnetic dipoles using A_{aniso}

$$R = \sqrt[3]{\frac{g\beta g_N\beta_N\mu_0 10^{-7}}{hA_{\mathrm{aniso}}}} \tag{4}$$

would give an *R* of about 1.8 Å, which is below the lowest limit of the applicability of the point dipole approximation because the electron density distribution cannot be neglected at such short distance.

4. Discussion

The satellites observed in a-Si:H and μc-Si:H after electron bombardment are ascribed to a hydrogen induced hyperfine pattern based on the results of the isotope exchange experiment. The finding is surprising because none of the available earlier works on MeV electron bombardment reported on the satellites in the spectra of a-Si:H or μc-Si:H [44–49]. We assume that the combination of the experimental conditions (2 MeV electron bombardment at about 100 K, chosen dose and dose accumulation rate, storage of the bombarded samples in LN_2) may be responsible for the fact that H-related paramagnetic states were observed in our studies.

The structure of the observed H-related paramagnetic complex cannot be determined from the available experimental data directly. Moreover, due to the inhomogeneous broadening and overlap of the hyperfine pattern with the resonance of the dangling bonds, the parameters of the *g*-tensor and hyperfine *A*-tensor are also not accessible directly. Simulation of the hyperfine spectra with available data of hydrogen-related centers in Si did not allow unambiguous identification of the measured resonance with a known H-related defect. On the other hand, we were able to simulate the measured spectrum of a possible hyperfine doublet by an axially symmetric powder pattern with parameters of the *g*- and *A*-tensors as listed in table 1 for the optimized *hfs(B)*.

According to the parameters of the optimized hfs(B), the corresponding center should have both isotropic and anisotropic hyperfine constants A_{iso} and A_{aniso} higher than any of the reported H-related centers in Si; i.e., an electron has to be localized closer to the H nuclei in this case. Although there is no center among those listed in table 1 which would have a set of parameters satisfactorily close to the parameters of optimized hfs(B), we note that two of them, BC-H (AA9) and H–db, have the closest similarities with the optimized hfs(B); see figure 4(a) and table 1.

Bond centered H (AA9), which is a donor state in c-Si [14], has a similar anisotropy of the A-tensor ($A_{iso}/A_{aniso} = 0.37$ versus 0.38 for optimized hfs(B)) but all values of the g-tensor are considerably lower than needed to fit the experimental data. Roughly speaking, in order to match the observed satellites, the AA9 center would have to be a deeper state with higher principal values of the g-tensor in the a-Si:H matrix than what is reported for this state in c-Si.

The bond centered H complex was observed in c-Si after 7 MeV proton implantation at 80 K. High energy protons are incorporated in the c-Si lattice and at low temperature form Si–H–Si complexes, which already anneal completely at 200 K. The formation and annealing of the bond centered H complex are qualitatively in line with the behavior of the H-related centers observed in the present study. 2 MeV electron bombardment performed at about 100 K creates defects partially by atomic displacements [50]. We can speculate that Si–H–Si centers can be created as a result of such H displacement, similarly to the creation of these states in H-implanted crystalline silicon.

As for the temperature stability, the observed hyperfine doublet shows faster reduction of the intensity than the central db resonance upon annealing [31]. However, complete annealing of the satellites takes place at 120–160 °C [30], which implies much higher stability of the corresponding H-related states in amorphous tissue in comparison to bond centered hydrogen in crystalline Si.

The second center of interest is the H-related db, which has similar g-tensor values but much higher A-tensor anisotropy than our optimized hfs(B) ($A_{iso}/A_{aniso} = 0.6$ versus $A_{iso}/A_{aniso} = 0.38$ for optimized hfs(B)). To match the parameters of the optimized hfs(B), the $A_{\parallel}$ and $A_{\perp}$ values of H–db have to be exchanged. In order to understand the relevance of such adjustment, the accuracy and reliability of the parameters of both optimized hfs(B) and H–db have to be taken into account. The existence of H-related db in a-Si:H has been suggested on the basis of the small difference between the db-resonance shapes before and after the light soaking [32, 33]. This difference has been used for powder pattern simulation and further estimation of the parameters of the H–db complex. Unfortunately, there were no isotope effect experiments performed to support the claimed role of H, and the broad featureless spectra allow for considerable freedom during the simulation. In view of this, we see the resonance parameters deduced from our simulation for the optimized hfs(B) as not in contradiction with the results of reference [32, 33].

Interestingly, both centers H–db and bond centered hydrogen (AA9) are included in prominent models of metastability in a-Si:H [5, 6]. Identification and detailed information on the properties of such states may provide grounds for further development of the metastability theory. As a matter of speculation, the H-related center found in the present study may appear to be the equivalent of the short lived intermediate state for H, theoretically predicted to exist during production and stabilization of metastable dbs in a-Si:H, although the particular structure of this center cannot be determined with the available data.

5. Conclusions

Hydrogen-related paramagnetic states have been investigated with ESR in equivalent hydrogenated and deuterated thin film silicon after 2 MeV electron bombardment performed at 100 K. The satellite-like features found in the spectra of a-Si:H and μc-Si:H after electron bombardment have not been resolved in the corresponding deuterated material. From the evident effect of H → D substitution, we conclude that the satellites can be ascribed to a hydrogen induced hyperfine pattern in e-bombarded a-Si:H and μc-Si:H.

Comparison of known H-related centers in c-Si and proposed H-related db in a-Si:H to the hyperfine pattern observed in the study has been performed by means of powder pattern simulations. Even though an unambiguous identification is not possible, we find reasonable agreement for bond centered hydrogen and an H–db complex proposed for a-Si:H and we are able to simulate the experimental spectra with very good agreement for a hyperfine pair with axially symmetric g- and A-tensors.

Acknowledgments

The authors acknowledge Andreas Lambertz for the assistance during material deposition, Markus Hülsbeck for the Raman measurements, Ivan Nekliudov for the support of the e-bombardment experiments, and Vladimir Smirnov and Matthias Fehr for helpful and stimulating discussions. The study has been carried out with financial support from the Science and Technology Center in Ukraine (STCU project No 655A) and the German Ministry of Education and Research (BMBF) within the network project ‘EPR-Solar’ (03SF0328).

Appendix

The powder pattern simulation has been performed with the ‘pepper’ function of the software tool *EasySpin* used for the simulations of the ESR spectra of disordered solids [42]. Principal values of g-tensor and A-tensor for each given H-related state have been taken from the literature and summarized in table 1. However, not every detail needed for the complete powder pattern simulation can be found in the literature. There are several assumptions to be made in order to conduct the simulations.

Structural disorder in a-Si:H leads to the scatter of the principal values of the g-tensor and A-tensor called ‘strain’, which is a reason for the inhomogeneous broadening of the

spectra in disordered solids. Both *g*-strain and *A*-strain lead to Gaussian shape of the resonance of a given spin packet in the powder spectrum. The width of the resonance of the individual spin packet may be determined by *g*-strain or *A*-strain, depending on which is stronger, but the effect of either on the linewidth of a spin packet is essentially the same. Here we took the *g*-strain to be dominant and therefore the inhomogeneous broadening in the simulated spectrum is given in terms of *g*-strain. Note that equivalent results are obtained with a dominant *A*-strain. Whenever possible, the *g*-strain values have been taken from the literature; however, in most cases there is no information on the degree of *g*-strain in a-Si:H for a given center found in crystalline Si. In these cases, a *g*-strain of 0.0043 has been used. This value is based on the fact that the sharpest features in the spectrum can be represented closely by the Gaussian line with a linewidth corresponding to the *g*-strain of 0.0043. Lower values of the *g*-strain are unlikely because sharper features would have been present in the spectrum. However, the components with higher *g*-stain cannot be excluded. It is assumed that there is no angular dependence of the *g*-strain, i.e. all spin packets in the powder spectrum experience equal inhomogeneous broadening, unless otherwise mentioned in the literature [32, 33].

Both *g*-tensor and *A*-tensor are assumed to be collinear.

The transition probability for all orientations in the powder pattern is assumed to be constant.

References

[1] Street R A 1991 *Hydrogenated Amorphous Silicon* (Cambridge: Cambridge University Press)
[2] Staebler D L and Wronski C R 1977 *Appl. Phys. Lett.* **31** 292
[3] Lang D V, Cohen J D and Harbison J P 1982 *Phys. Rev. Lett.* **48** 421
[4] Shimizu T 2004 *Japan. J. Appl. Phys.* **43** 3257
[5] Stutzmann M, Jackson W B and Tsai C C 1985 *Phys. Rev.* B **32** 23
[6] Branz H M 2003 *Sol. Energy Mater. Sol. Cells* **78** 425
[7] Fehr M, Schnegg A, Rech B, Lips K, Astakhov O, Finger F, Pfanner G, Freysoldt C, Neugebauer J, Bittl R and Teutloff C 2011 *Phys. Rev.* B **84** 245203
[8] Pfanner G, Freysoldt Ch, Neugebauer J and Gerstmann U 2012 *Phys. Rev.* B **85** 195202
[9] Weil J A and Bolton J R 2007 *Electron Paramagnetic Resonance: Elementarytheory and Applications* (New Jersey: Wiley) pp 99–105
[10] Stein H J 1971 *Radiat. Eff. Defect Solids* **9** 195
[11] Watkins G D 2000 *Mater. Sci. Semicon. Proc.* **3** 227
[12] Schweiger A 1993 *Appl. Magn. Reson.* **5** 229–64
[13] Mohr P J, Taylor B N and Newell D B 2008 *Rev. Mod. Phys.* **80** 633–730
[14] Gorelkinskii Yu V and Nevinnyi N N 1991 *Physica* B **170** 155
[15] Bech Nielsen B, Johannesen P, Stallinga P, Bonde Nielsen K and Byberg J R 1997 *Phys. Rev. Lett.* **79** 1507
[16] Johannesen P, Bech Nielsen B and Byberg J R 2000 *Phys. Rev.* B **61** 4659
[17] Stallinga P, Gregorkiewicz T, Ammerlaan C A J and Gorelkinskii Yu V 1993 *Phys. Rev. Lett.* **71** 117
[18] Miyagawa I and Gordy W 1961 *J. Am. Chem. Soc.* **83** 1036
[19] Biegelsen D K and Stutzmann M 1986 *Phys. Rev.* B **33** 3006
[20] Stutzmann M and Biegelsen D K 1989 *Phys. Rev.* B **40** 9834
[21] Ishii N, Kumeda M and Shimizu T 1982 *Japan. J. Appl. Phys.* **21** L92
[22] Yamasaki S and Isoya J 1993 *J. Non-Cryst. Solids* **164** 169
[23] Isoya J, Yamasaki S, Okushi H, Matsuda A and Tanaka K 1993 *Phys. Rev.* B **47** 7013
[24] Isoya J, Yamasaki S, Matsuda A A and Tanaka K 1994 *Phil. Mag.* B **69** 263
[25] Lim P K, Tam W K, Yeung L F and Lam F M 2007 *J. Phys.: Conf. Ser.* **61** 708
[26] Yamasaki S, Kuroda S, Tanaka K and Hayashi S 1984 *Solid State Commun.* **50** 9
[27] Brandt M S, Bayerl M W, Stutzmann M and Graeff C F O 1998 *J. Non-Cryst. Solids* **227** 343
[28] Fehr M, Schnegg A, Teutloff C, Bittl R, Astakhov O, Finger F, Rech B and Lips K 2010 *Phys. Status Solidi* a **207** 552
[29] Astakhov O, Carius R, Petrusenko Yu, Borysenko V, Barankov D and Finger F 2007 *Phys. Status Solidi (RRL)* **2** R77
[30] Astakhov O, Finger F, Carius R, Lambertz A, Petrusenko Yu, Borysenko V and Barankov D 2007 *Thin Solid Films* **515** 7513
[31] Astakhov O, Carius R, Lambertz A, Petrusenko Yu, Borysenko V, Barankov D and Finger F 2008 *J. Non-Cryst. Solids* **354** 2329
[32] Hikita H, Takeda K, Kimura Y, Yokomichi H and Morigaki K 1997 *J. Phys. Soc. Japan* **66** 1730
[33] Takeda K, Hikita H, Kimura Y, Yokomichi H and Morigaki K 1998 *Japan. J. Appl. Phys.* **37** 630
[34] Baia Neto A L, Lambertz A, Carius R and Finger F 2002 *J. Non-Cryst. Solids* **299** 274
[35] Dylla T 2005 *Electron Spin Resonance and Transient Photocurrent Measurements on Microcrystalline Silicon* vol 43 (Jülich: Forschungszentrum Jülich GmbH) Schriften des Forschungszentrums Jülich, Energietechnik
[36] Houben L, Luysberg M, Hapke P, Carius R, Finger F and Wagner H 1998 *Phil. Mag.* A **77** 1447
[37] Astakhov O, Carius R, Petrusenko Yu, Borysenko V, Barankov D and Finger F 2007 *Mater. Res. Soc. Symp. Proc.* **989** 3
[38] Astakhov O, Carius R, Finger F, Petrusenko Yu, Borysenko V and Barankov D 2009 *Phys. Rev.* B **79** 104205
[39] Finger F, Carius R, Dylla T, Klein S, Okur S and Günes M 2003 *IEE Proc. Circ. Dev. Syst.* **150** 300
[40] Taylor P C, Baugher J F and Kriz H M 1975 *Chem. Rev.* **75** 203
[41] Poole C P and Farach H A 1979 *Bull. Magn. Reson.* **1** 162
[42] Stoll S and Schweiger A 2006 *J. Magn. Reson.* **178** 42–55
[43] Rodgers J L and Nicewander W A 1988 *Am. Stat.* **42** 59
[44] Street R, Biegelsen D and Stuke J 1979 *J. Phil. Mag.* B **40** 451
[45] Voget-Grote U, Kümmerle W, Fischer R and Stuke J 1980 *Phil. Mag.* B **41** 127
[46] Pontuschka W M, Carlos W W, Taylor P C and Griffith R W 1982 *Phys. Rev.* B **25** 4362
[47] Dersch H, Schweitzer L and Stuke J 1983 *Phys. Rev.* B **28** 4678
[48] Dersch H, Skumanich A and Amer N M 1985 *Phys. Rev.* B **31** 6913
[49] Bronner W, Mehring M and Brüggemann R 2002 *Phys. Rev.* B **65** 165212
[50] Vavilov V S and Ukhin N A 1977 *Radiation Effects in Semiconductors and Semiconductor Devices; Translated From Russian* (New York: Consultants Bureau)